Polymer Films on Electrodes

XXIV. Ellipsometric Study of the Electrochemical Redox Processes of a Polypyrrole Film on a Platinum Electrode

Chongmok Lee, Juhyoun Kwak, and Allen J. Bard*

Department of Chemistry, The University of Texas, Austin, Texas 78712

ABSTRACT

Ellipsometry was used to observe the *in situ* growth and electrochemical conversion redox processes of a polypyrrole film, which was electrochemically deposited to a thickness of *ca.* 100 nm on a platinum electrode in 0.2*M* KCl solution containing 50 m*M* pyrrole. To determine the spatial distribution of oxidized and reduced states during the reduction and oxidation of the film, the conversion process was simulated by a multilayer film model. Such simulations of the ellipsometric results show that the redox conversion of a polypyrrole film proceeds from the solution toward the electrode and is controlled by counterion movement. These results contrast with previous work on a thionine film where conversion proceeds from electrode to solution. The effective diffusion constant for charge transport based on ellipsometric simulation was estimated as 1.7×10^{-10} cm^2/s.

We describe ellipsometric studies of the growth and redox processes in a film of the electronically conducting polymer, polypyrrole, and show how these measurements can provide information about film thickness and the mechanism of the interconversion between the oxidized and reduced states. There have been numerous recent studies of electronically conducting polymers (1) because of potential applications of these materials (*e.g.*, in displays, batteries, and molecular electronic devices) as well as interest in the inherent properties and mechanism of conduction. The redox processes in polypyrrole have been mainly investigated by electrochemical methods, such as ac impedence methods (2, 3), chronocoulometry (3, 4), and cyclic voltammetry (5). Because the material is a good electronic conductor in its oxidized state, the rates of oxidation and reduction are thought to be limited by counterion motion within the polymer film (6). Although there have been numerous studies of preparation and behavior of polypyrrole films, few papers have been concerned with ellipsometric observations (3, 7). We show in this study that the direction of the redox conversion process inside the polypyrrole film is from the solution to the substrate. These results complement our previous study (8), where we found the reverse direction for the conversion processes in a thionine film. To determine how conversion of the film from the oxidized (O) to the reduced (R) state (or the reverse process) occurs in terms of the spatial distribution of O and R during the process, the ellipsometric data for partial reduction and reoxidation of the film were analyzed by simulating the processes in terms of a stratified planar isotropic multilayer model (8, 9).

Electrochemical film conversion processes are frequently associated with significant variations in optical properties of the film. Such ellipsometric studies can provide mechanistic information about charge transport by measurements with a film grown to a given thickness as it is electrochemically oxidized and reduced (10). Other ellipsometric/electrochemical studies of polymer films include polyaniline (10), poly(vinylferrocene) (11), thionine (8), and polymeric viologen (12). Similar studies have been carried out on the reduction processes in metal oxide films (13, 14).

Three modes of oxidative or reductive conversion of the film are usually considered (8, 10-14). These depend upon the rate of charge (electron and ion) propagation through the film and the experimental conditions. (A) If the charge mobilities are high and the sampling time long, the conversion of the film appears spatially uniform; *i.e.*, the O and R concentrations are not functions of the distance, x, into the film from the substrate surface (15). (B) If electron mobility through the film is larger than ion mobility, conversion occurs from the film/solution interface toward the substrate electrode/film interface. (C) If ion mobility is larger than electron mobility, conversion proceeds in the reverse direction of (B). Earlier studies (10, 11, 13, 14) considered these alternatives (case B and C) and derived the ellipsometric behavior based on a two-layer model of the film. In the polyaniline study (10), spatially uniform conversion (case A) was found. In our previous work on the thionine film (8), the conversion process was simulated by a multilayer film model (8, 9, 16, 17) with up to eight or nine discrete film layers considered. The redox conversion of a thionine film was shown to proceed from the electrode/film interface toward the solution using the Nernst diffusion layer approach (18). In this study a similar multilayer film model is used for a polypyrrole film. We also estimate the effective diffusion coefficient for charge transport based on the simulated results, using an approach analogous to that used in spectroelectrochemistry (19).

*Electrochemical Society Active Member.

Experimental

Experimental details about the optical cell and the ellipsometry apparatus are given elsewhere (8, 20). The characteristic sampling time for obtaining the ellipsometric parameters, Ψ and Δ, during the measurement of redox conversion was 37 ms. The Pt disk electrode (area 0.176 cm^2) was mounted in the bottom of a Teflon cell that contained an auxiliary (Pt gauze) and reference (saturated calomel electrode [SCE]) electrodes and was polished to an optically flat condition before the deposition of polypyrrole (all polishing supplies from Buehler, Limited). The film deposition was accomplished by cyclic potential sweeps between 0.70 and −0.25V *vs.* SCE in an aqueous solution containing 50 m*M* pyrrole (Aldrich, Milwaukee, Wisconsin) in 0.2*M* KCl in the optical cell at a sweep rate of 100 mV/s. Ellipsometric measurements were undertaken *in situ* during the film growth and those of the redox conversion of the deposited film were performed after the solution containing monomer was replaced by an aqueous 0.2*M* KCl solution. Ellipsometric measurements of film growth during film deposition and film conversion were made at a wavelength of 632.8 nm (He-Ne laser) and an angle of incidence of 67°.

Results and Discussion

Polypyrrole film growth.—Polypyrrole film growth on a Pt electrode was monitored by making *in situ* ellipsometric measurements while continuously cycling the potential between 0.70 and −0.25V *vs.* SCE at 100 mV/s in an aqueous solution containing 50 m*M* pyrrole and 0.2*M* KCl. Two sets of 26 measurements of the ellipsometric parameters, Ψ and Δ, were made at *ca.* 0.70V *vs.* SCE (the oxidized state) and −0.25V *vs.* SCE (the reduced state), respectively, during the potential sweeps. This technique can be employed to determine *in situ* redox states and film thickness when the solution used for film deposition is optically transparent at the wavelength of the light source (12, 20, 21). We chose a cyclic sweep growth mode rather than a potentiostatic growth mode, because the former produced better films (12). Typical results of film growth are shown

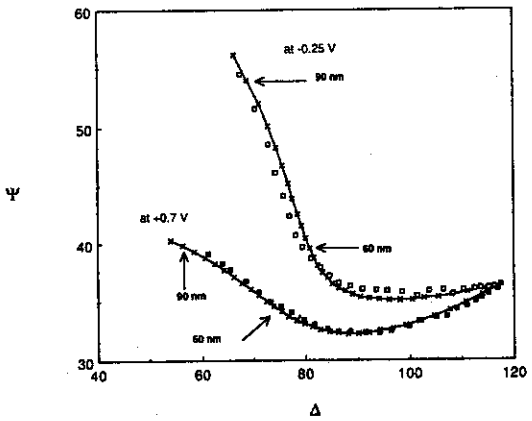

Fig. 1. Experimental and calculated ellipsometric data for the growth of a polypyrrole film on a Pt disk electrode. Curved lines are calculated assuming a uniform refractive index: 1.60-0.46i for the oxidized form (lower curve) and 1.72-0.27i for the reduced form (upper curve). Square points show experimental ellipsometric data: ■ for oxidized form (at 0.7V vs. SCE), □ for reduced form (at −0.25V vs. SCE). 'X' represents calculations for every 3 nm thickness.

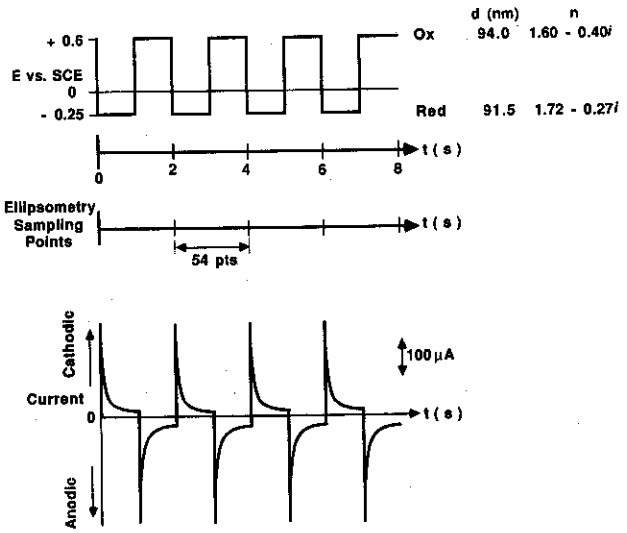

Fig. 2. Schematic diagram of experimental conditions for measurements of conversion processes.

in Fig. 1. The ellipsometric growth curves could be fit very closely over a range of thicknesses of up to 90 nm by using a refractive index, n, of 1.60-0.46i for the oxidized form (n_O) and 1.72-0.27i for the reduced form (n_R) at 632.8 nm. As expected for a metallic conductor, the imaginary part of n_O, 0.46, at 0.70V *vs.* SCE is unusually large for an organic material. The real part of n_O is smaller than that of n_R. A similar tendency was also noted in the galvanostatic growth of polypyrrole in a $NaClO_4$ electrolyte at 546.1 nm, *i.e.*, 1.47-0.39i(n_O) at 0.50V and 1.56-1.17i(n_R) at −0.3V *vs.* SCE (3). Note, however, that Arwin *et al.* (7) report an imaginary part of n_O of the order of 0.2 using $(C_2H_5)_4NBF_4$ from spectroellipsometric measurements in the λ range 1.5-6 eV, and that the anion, which serves as a counterion in the oxidized film, does influence both the structural properties and electroactivities of the films (22).

Redox conversion.—The interconversion between the redox states in 0.2*M* KCl in the absence of monomer was studied with a film grown to a thickness of *ca.* 90 nm. The cell containing the film grown in 0.2*M* KCl and 50 m*M* pyrrole was removed from the ellipsometer, the growth solution was removed, and the cell was washed and then filled with 0.2*M* KCl alone. When the cell was replaced on the ellipsometer, the value of Ψ had shifted from 40° to 42°, because of a small change in cell geometry or film state. Interconversion was then studied by measurement of the ellipsometric parameters, Ψ and Δ, every 37 ms during the application multiple potential steps (*i.e.*, four cycles of a double potential step) from an initial potential of 0.6 to −0.25V for a 1s pulse width (Fig. 2). Because of the small shift in Ψ, it was necessary to use as the imaginary part of n_O a value of 0.40 rather than 0.46, to simulate the experimental interconversion curves. Results of representative data points in such potentiostatic experiments for an oxidized film 94.0 nm (d_O) thick at 0.60V *vs.* SCE and the reduced film 91.5 nm (d_R) thick at −0.25V *vs.* SCE are shown in Fig. 3. One disadvantage in the study of polypyrrole films for such conversion processes compared with thionine films is the larger effective diffusion coefficient for charge transport, D_E, for polypyrrole of the order of 10^{-9}-10^{-10} cm^2/s in Cl^- and ClO_4^- (3, 4), as compared to 10^{-12} cm^2/s for thionine (23). This makes the rate of interconversion much faster so that it is difficult to keep track of the conversion curve with an ellipsometer with a relatively long sampling time (8). To overcome this problem we employed multiple cycles of double potential steps (12). The use of potential steps rather than the cyclic potential sweeps for the interconversion (8, 11, 22a) simplified the simulations and permitted the calculation of D_E from the experimental data.

In Fig. 3 experimental ellipsometric data are consistent with a multilayer model D in which the conversion of the film begins at the solution/film interface and proceeds toward the electrode/film interface. Other possible models are given for comparison purposes. Details will be discussed later.

Simulations.—To determine the spatial distribution of O and R during the reduction and oxidation of the film, the refractive index change and thickness change must be incorporated into a simulation according to models A, B, or C. The refractive indexes and thicknesses of O and R at the two limiting states between the interconversion processes

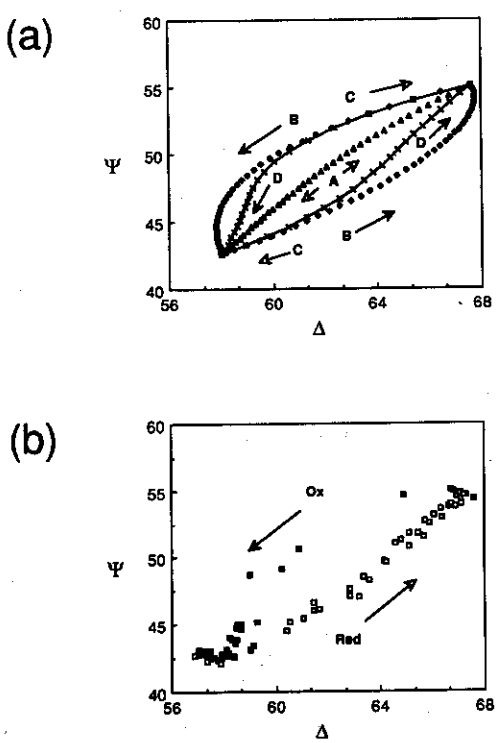

Fig. 3. (a) Simulated and (b) experimental ellipsometric conversion data of polypyrrole film deposited on a Pt disk electrode in 0.2*M* KCl solution, recorded at 632.8 nm at a 67° angle of incidence during multipotential step (pulse width, 1s) between 0.6 and −0.25V *vs.* SCE. Simulated at 0.6V; $n_O = 1.60 - 0.40i$; $d_O = 94.0$ nm; at −0.25V, $n_R = 1.72 - 0.27i$, $d_R = 91.5$ nm. Simulated curves A, B, C, and D correspond to the respective conversion model (see text): Δ for A, ◇ for B and C, -x- for D, and open and closed squares for representative experimental data.

(n_O, n_R, and d_O, d_R) were given earlier. Different simulated redox conversion curves were obtained for model A (uniform conversion), model B (from solution to substrate), and model C (from substrate to solution). In the latter two cases, the film was simulated by a two-layer model, as in previous cases (8, 10, 13, 14) and also by equivalent multilayer models [models D and E (8)] as shown schematically in Fig. 4. The following considerations hold for the different models. In the homogeneous film model (A), n and d are taken to vary uniformly with the fractional extent of conversion, f, where f = (charge passed)/(total charge for conversion between the two limiting redox states). For models B and C (two-layer simulation), two homogeneous films with refractive indexes n_O and n_R are assumed with relative thicknesses a linear function of f and an orientation of O and R layers determined by the model and the direction of reaction. For models A, B, and C, simulations were carried out for 40 steps representing different stages of conversion for each redox conversion process. The multilayer models are analogous to those in our previous report (8).

For the multilayer model D, 20 steps indexed by i and representing different degrees of the film conversion were employed to represent the oxidation and 20 steps to represent the reduction. A Nernst diffusion layer approach (18) inside the polymer film from the solution/film interface toward the electrode/film interface was used, where the thickness of the diffusion layer at different stages of the conversion was taken to be i/10 of the total film thickness ($i < 10$). This growing diffusion layer was divided into eight discrete sublayers to make a step-function concentration profile reflecting a linear diffusion profile. Each sublayer, indexed by j, had a thickness d_{ij} and a refractive index n_{ij}. The refractive index of each stage, i, in layer j was taken to be proportional to the fractional concentrations of O and R in layer j, $f_{O,ij}$ and $f_{R,ij}$, respectively, and the bulk refractive indexes, n_O and n_R; *i.e.*

$$n_{ij} = f_{O,ij}n_O + f_{R,ij}n_R \quad [1]$$

$$n_{ij} = f_{O,ij}n_O + (1 - f_{O,ij})n_R \quad [2]$$

For example, for the reduction process (when O is converted to R), when the thickness of the growing diffusion layer was smaller than the thickness of the film (taken arbitrarily for i = 1-9, where i/20 is the degree of conversion), the fractional concentration of the O state in layer j at step i was

for

$$i = 1 \text{ to } 9 \quad f_{O,i1} = 1 \quad (\text{for } j = 1) \quad [3a]$$

$$f_{O,i1} = [1 - (2j - 3)/16] \quad (\text{for } j = 2\text{-}9) \quad [3b]$$

where the thickness of layer j at stage i was taken as

$$d_{i1} = [1 - (i/10)]d_O \quad (\text{for } j = 1) \quad [4a]$$

$$d_{ij} = f_{O,ij}(i/10)(d_O/8) + (1 - f_{O,ij})(i/10)(d_R/8)$$

$$(\text{for } j = 2\text{-}9) \quad [4b]$$

This adjustment of the simulation layer thickness with extent of oxidation was incorporated, because d_O is not equal to d_R. After the thickness of the growing diffusion layer attained that of the film (i = 10-19), $f_{O,ij}$ was taken as

$$\text{for } i = 10\text{-}19 \quad f_{O,ij} = [1 - (2j - 1)/16][1 - (i - 10)/10]$$

$$(\text{for } j = 1\text{-}8) \quad [5]$$

where the thickness of each j^{th} layer is given by

$$d_{ij} = f_{O,ij}(d_O/8) + (1 - f_{O,ij})(d_R/8) \quad (\text{for } j = 1\text{-}8) \quad [6]$$

This procedure allows simulation of the experimental results (Ψ and Δ) based on the approach used in ellipsometry for stratified planar isotropic structures (9, 16, 17). We consider a stratified structure that consists of a stack of $1, 2 \ldots j$(j = 8 or 9 in this study as shown in the previous equations) parallel layers sandwiched between two semi-infinite phases; the bulk solution and the substrate electrode. A scattering matrix, S, can be expressed as a product of the interface, and layer matrices, I and L, that describe the effects of the individual interfaces and layers of the entire stratified structure, taken in proper order, as follows (9)

$$S = I_{01}L_1I_{12}L_2\ldots\ldots I_{(j-1)j}L_jI_{j(j+1)} \quad [7]$$

where I and L are used as defined in Ref. (8). By solving the above equation, with the refractive indexes and film thicknesses of the oxidized and reduced forms (n_O, n_R, and d_O, d_R), simulation results can be obtained without any adjustable parameters.

Simulations of the ellipsometric results according to the different models are shown in Fig. 3 and 5. For the simplest models (A, B, C), the conversion follows most closely that for model B, but shows large deviations from that model, especially at the later stages of both the oxidation and reduction processes; compare Fig. 3a and b. A much better fit is obtained with the multilayer model D, which assumes the same direction of the conversion processes (Fig. 5). Although this multilayer model uses a simplified linear diffusion layer approach to determine the concentration profile with eight or nine discrete layers rather than a more rigorous simulation of the concentration profiles, the results are in good agreement with the experimental data, so that these methods appear adequate, as also sug-

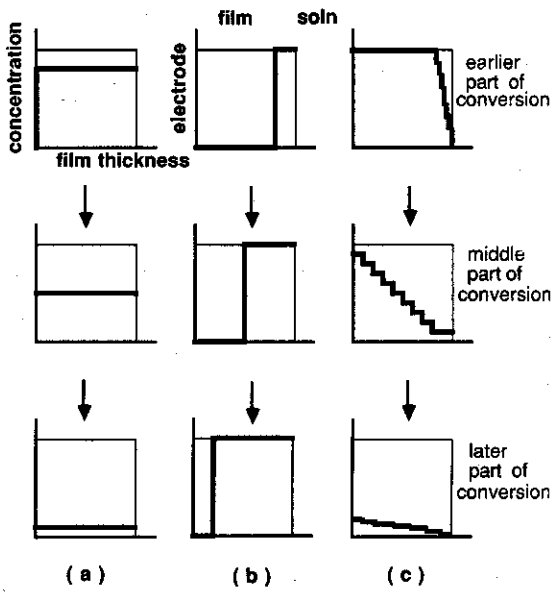

Fig. 4. Schematic diagram for the three conversion models: (a) homogeneous film conversion model (model A in text), (b) two-layer conversion model (from solution/film toward electrode/film (model B in text), and (c) multilayer conversion model (model D in text).

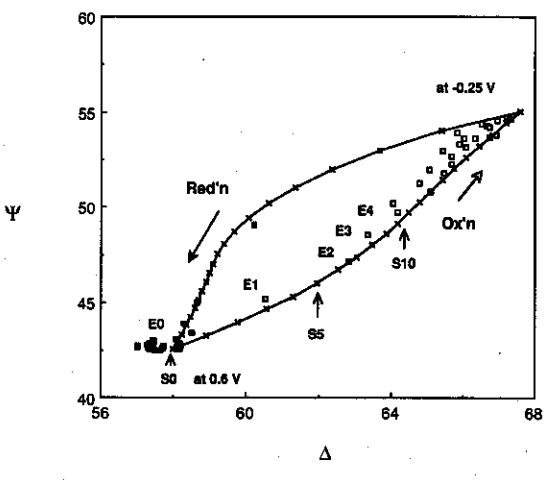

Fig. 5. Overlap plot of simulated curve (from model D) (X) and the experimental data (□ and ■) during one cycle of a double potential step. The points marked E_i and S_i are those used in determination of D_E (see text).

gested by previous results with a thionine film (8). There have been numerous studies of redox processes and modes of charge transport in polymer films (15). The rates of these processes are frequently governed by either the rate of electron transport through the film, *e.g.*, by electron hopping from one electroactive site to another or by physical diffusion of electroactive species in the film, or the rate of counterion motion within the film. Which of these processes is faster determines the direction in which a film redox process occurs with respect to the substrate/film and film/solution interfaces. For many polymer films, such as the ionomers and the thionine film previously studied, electron transfer appears to be rate-limiting, so that redox processes start at the substrate/film interface and propagate outward. For a good electronic conductor, such as polypyrrole, at least in its oxidized state, counterion movement is the slower process, and the redox process starts at the film/solution interface and propagates inward (10, 24, 25). The same process direction appears to occur with the less conductive reduced form of polypyrrole during its oxidation. Note that previous reports have also suggested rate-limiting ion movement, diffusion of counter anion (22a), or cation (26) and/or migration of counterion (6) in such films. Finally, we should point out that previous studies of polypyrrole films suggest that they are not dense uniform ones, but rather consist of a fibrous and highly porous structure (2a, 27). Thus, the model used here, which considers the film layers in terms of a single refractive index, represents an "effective medium" approximation of the kind frequently used in ellipsometric studies (9, 10, 21).

Estimation of D_E.—A value for the effective diffusion coefficient of charge transport in the film, D_E, can be obtained from the ellipsometric results by assuming that the electrochemical and electrochromic processes occur simultaneously as in spectroelectrochemical studies. For this purpose, an overlap plot of the simulated curve (from model D) and all of the experimental data (rather than the representative points) during one cycle of the double potential step (shown in Fig. 5) was made. The early part of the reduction process in Fig. 5 will be employed to demonstrate the derivation of D_E in terms of ellipsometric behavior because of the relatively good fit of the simulated points with the experimental data and relatively uniform intervals between the simulated points. We assign the experimental data ('□' symbols in Fig. 5) as E_0, E_1.....E_4 from the left to the right and the simulated data ('X' symbols in Fig. 5) as S_0, S_1.....S_{10}. The time interval (the characteristic sampling time) between E_k and E_{k+1} (for k = 0-3) is 37 ms. However, because the ellipsometric measurements were not synchronized with the potential application, there is an arbitrary time-delay, t_d, between 0 and 37 ms, between the application of the potential step, and the recording of the first experimental ellipsometric point. At each S_i point ($i \leq 10$), the thickness of the approximately linear diffusion layer (step function), $d(s_i)$, is

$$\delta(t) \approx d(s_i) = \Sigma d_{ij} \quad (\text{from } j = 2\text{-}9) \qquad [8]$$

where d_{ij} is defined in Eq. [4b]. Therefore, the approximate thickness of the diffusion layer at each E_k (for k = 1-4) obtained in this way is $\delta(t)$ as given by the Nernst approximation (18). D_E can be estimated from Eq. (9), if t_d is known

$$\delta(t) = 2(D_E t)^{1/2} \qquad [9]$$

Plots of $\delta(t)$ *vs.* $t^{1/2}$ were made with different values of t_d until a linear plot with zero intercept was obtained (Fig. 6). This plot yielded an estimated value of D_E of 1.7×10^{-10} cm²/s. This can be compared to reported D_E values in ClO_4^- of 6.2×10^{-10} cm²/s (4) and in Cl^- and ClO_4^-, 3×10^{-9} and 3.1×10^{-9} cm²/s, respectively (3). Note that even this simplified spectroelectrochemical (19) approach yields a reasonable approximation for D_E.

The results in Fig. 5 suggest that the oxidation process occurs somewhat faster than the reduction process, although the simulated points during oxidation are concentrated near the fully oxidized state. Previous work (22a) reported that the switching rate between the redox states is very sensitive to the nature of the anion, and, in general,

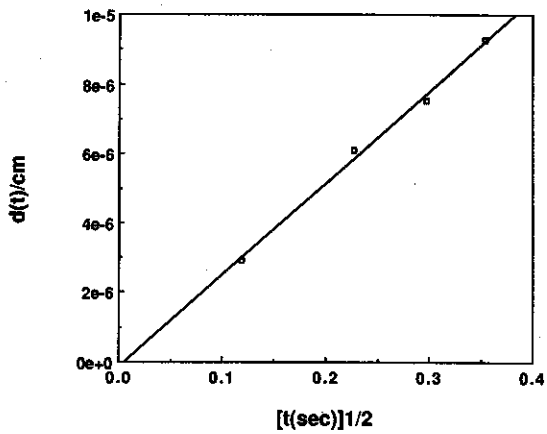

Fig. 6. Plot $\delta(t)$/cm *vs.* $[t(s)]^{1/2}$ based on data in Fig. 5, with t_d = 22 ms

that the rate of oxidation is slightly higher than the rate of reduction.

Conclusions

An ellipsometric study of the mode of spatial propagation of oxidized and reduced sites inside a polypyrrole film based on a diffusion-limited redox conversion multilayer simulation suggests that the direction of this process is from the solution/film interface toward the electrode/film interface. This conversion direction is consistent with ion transport (rather than electron transfer) being the rate-limiting process as reported in other studies (6, 22, 26). This conversion is the reverse of that found in a previous ellipsometric study of a thionine film (8), where the conversion was an electron-transfer rate-limiting process (10). These studies demonstrate the validity of the ellipsometric approach to distinguish between these two alternatives experimentally for organic polymer films. This study also demonstrates that an approximate diffusion constant for charge transport can be estimated by ellipsometry. We report a D_E value of 1.7×10^{-10} cm²/s, which is similar to values obtained by other techniques (3, 4).

Acknowledgments

The support of this research by the National Science Foundation (CHE 8402135) is gratefully acknowledged. We thank Larry Kepley for his rapid data acquisition program.

Manuscript submitted March 31, 1989; revised manuscript received *ca.* May 1, 1989.

The University of Texas assisted in meeting the publication costs of this article.

REFERENCES

1. See, for example, (a) "Handbook of Conducting Polymers," Vol. 1, T. A. Skotheim, Editor, Marcel Dekker, New York (1986); (b) J. E. Frommer and R. R. Chance, *Encycl. Polym. Sci. Eng.*, **5**, 462 (1986); (c) A. F. Diaz, *Chem. Scripta*, **17**, 145 (1981).
2. (a) R. A. Bull, F.-R. F. Fan, and A. J. Bard, *This Journal*, **129**, 1009 (1982); (b) R. M. Penner and C. R. Martin, *J. Phys. Chem.*, **93**, 984 (1989).
3. F. T. A. Vork, Ph.D. Dissertation, Eindhoven University of Technology, Eindhoven, The Netherlands (1988).
4. E. M. Genies, G. Bidan, and A. F. Diaz, *J. Electroanal. Chem.*, **149**, 101 (1983).
5. E. M. Genies and J.-M. Pernant, *Synth. Met.*, **10**, 117 (1984/1985).
6. C. D. Paulse and P. G. Pickup, *J. Phys. Chem.*, **92**, 7002 (1988).
7. H. Arwin, D. E. Aspnes, R. Bjorklund, and I. Lundström, *Synth. Met.*, **6**, 309 (1983).
8. C. Lee, J. Kwak, L. J. Kepley, and A. J. Bard, Submitted to *J. Electroanal. Chem.*
9. R. M. A. Azzam and N. M. Bashara, "Ellipsometry and Polarized Light," North Holland, Amsterdam (1977).
10. (a) S. Gottesfeld, A. Redondo, and S. W. Feldberg, *This Journal*, **134**, 271 (1987); (b) S. Gottesfeld in "Electroanalytical Chemistry," Vol. 15, A. J. Bard, Editor,

Marcel Dekker, New York (1988).
11. G. C. Winston and C. M. Carlin, *This Journal*, **135,** 789 (1988).
12. L. J. Kepley, C. Lee, and A. J. Bard, Manuscript in preparation.
13. M. A. Hopper and J. L. Ord, *This Journal*, **120,** 183 (1973).
14. J. C. Clayton and D. J. DeSmet, *This Journal*, **123,** 174 (1976).
15. (a) R. W. Murray in "Electroanalytical Chemistry," Vol. 13, A. J. Bard, Editor, Marcel Dekker, New York (1984); (b) P. Daum, J. R. Lenhard, D. Rolison, and R. W. Murray, *J. Am. Chem. Soc.*, **102,** 4649 (1980).
16. R. H. Muller and C. G. Smith, *Surf. Sci.*, **56,** 440 (1976).
17. G. E. Jellison, Jr. and F. A. Modine, *J. Opt. Soc. Am.*, **72,** 1253 (1982).
18. A. J. Bard and L. R. Faulkner, "Electrochemical Methods: Fundamentals and Applications," Chap. 1, Wiley, New York (1980).
19. W. R. Heineman, F. M. Hawkridge, and H. N. Blount, in "Electroanalytical Chemistry," Vol. 13, A. J. Bard, Editor, Marcel Dekker, New York (1984).
20. L. J. Kepley and A. J. Bard, *Anal. Chem.*, **60,** 1459 (1988).
21. C. M. Carlin, L. J. Kepley, and A. J. Bard, *This Journal*, **132,** 353 (1985).
22. (a) A. F. Diaz and J. Bargon in "Handbook of Conducting Polymers," Vol. 1, T. A. Skotheim, Editor, Marcel Dekker, New York (1986), (b) M. Salmon, A. F. Diaz, A. J. Logan, M. Krounbi, and J. Bargon, *Mol. Cryst. Liq. Cryst.*, **83,** 1297 (1983).
23. W. J. Albery, M. G. Boutelle, P. J. Colby, and A. R. Hillman, *J. Electroanal. Chem.*, **133,** 135 (1982).
24. (a) S. Gottesfeld and J. D. E. McIntyre, *This Journal*, **126,** 742 (1979); (b) S. Gottesfeld, *ibid.*, **127,** 272 (1980).
25. K. Hutchinson, R. E. Hester, W. J. Albery, and A. R. Hillman, *Faraday Trans. 1*, **80,** 2053 (1984).
26. J. R. Reynolds, N. S. Sundaresan, M. Pomerantz, S. Basak, and C. K. Baker, *J. Electroanal. Chem.*, **250,** 355 (1988).
27. R. Yang, K. M. Dalsin, D. F. Evans, L. Christensen, and W. A. Hendrickson, *J. Phys. Chem.*, **93,** 511 (1989).

Reprinted from JOURNAL OF THE ELECTROCHEMICAL SOCIETY
Vol. 136, No. 12, December 1989
Printed in U.S.A.